EXPERIMENTAL

Joseph D. DiRocco
David E. Carney
Gary F. Nieman

Correlation between alveolar recruitment / derecruitment and inflection points on the pressure-volume curve

J. D. DiRocco (✉) · D. E. Carney · G. F. Nieman
Upstate Medical University, Department of Surgery,
750 E Adams Street, Syracuse 13210, NY, USA
e-mail: DiRoccoJ@upstate.edu
Tel.: +1-315-4646367
Fax: +1-315-4646294

Abstract *Objective:* To determine whether individual alveolar recruitment/derecruitment (R/D) is correlated with the lower and upper inflections points on the inflation and deflation limb of the whole-lung pressure-volume (P-V) curve. *Design and setting:* Prospective experimental study in an animal research laboratory. *Subjects:* Five anesthetized rats subjected to saline-lavage lung injury. *Interventions:* Subpleural alveoli were filmed continuously using an in vivo microscope during the generation of a whole-lung P-V curve using the super syringe technique. Alveolar R/D was correlated to the calculated inflection points on both limbs of the P-V curve. *Measurements and results:* There was continual alveolar recruitment along the entire inflation limb in all animals. There was some correlation ($R^2 = 0.898$) between the pressure below which microscopic derecruitment was observed and the upper inflection point on the deflation limb. No correlation was observed between this pressure and the lower inflection point on the inflation limb. *Conclusions:* In this physiological experiment in lungs with pure surfactant deactivation we found that individual alveolar recruitment measured by direct visualization was not correlated with the lower inflection point on inflation whereas alveolar derecruitment was correlated with alveolar derecruitment on deflation. These data suggest that inflection points on the P-V curve do not always represent a change in alveolar number.

Keywords Mechanical ventilation · Pressure-volume curves · Positive end-expiratory pressure · Acute lung injury · Ventilator-induced lung injury · Pulmonary alveoli

Introduction

It has been suggested that the inflection points on the whole-lung pressure-volume (P-V) curve could be used as a tool to determine when the lung is fully recruited and to set the optimal level of positive end-expiratory pressure (PEEP). Much attention has been given to the inflation limb of the P-V curve. The original hypothesis was that the majority of alveolar recruitment occurs at inflation pressures just above the lower inflection point on the inflation limb (LIP_i) of the P-V curve. Furthermore it was presumed that the lung was fully recruited at the upper inflection point of the inflation limb (UIP_i) [1]. According to this model, PEEP should be set above the LIP_i to prevent alveolar collapse, and peak inspiratory pressure should be set below the UIP_i to prevent alveolar overdistension. Mathematical models of alveolar opening [2–4], animal experimentation [5–7], and clinical studies [8, 9] have all challenged this hypothesis. These newer studies suggest that alveoli recruit along the entire inflation limb of the P-V curve, not merely at the LIP_i [3–7]. Recent understanding also suggests that to prevent alveolar recollapse it would be better to set PEEP in relation to the upper inflection point on the deflation limb (UIP_d) since

the UIP_d is the pressure below which significant alveolar derecruitment begins [9].

Both the animal [5–7] and clinical studies [8, 9] used indirect techniques to infer what was occurring at the alveolar level. In an earlier study we used in vivo microscopy to directly measure the inflation of individual subpleural alveoli on the inflation limb of the P-V curve and constructed pressure-alveolar area curves and compared them with the whole-lung P-V curve [6]. Our results demonstrated the tremendous complexity (i. e., change in size, shape, and number of alveoli) involved in alveolar recruitment that could not be measured with imaging modalities that assess only changes in lung density such as computed tomography [6].

In this study we hypothesized that the recruitment and derecruitment (R/D) of individual alveoli would correspond with the LIP on inflation and UIP on deflation. We used an in vivo microscopic technique to analyze alveolar R/D on *both limbs* of the P-V curve. In addition, we fit the P-V curve to a sigmoid equation [10], calculated both LIP and UIP on inflation and deflation, and correlated these inflection points with alveolar recruitment and derecruitment.

Methods

Study protocol

Following approval by the local animal ethics committee, eight male Sprague–Dawley rats (405–564 g) were anesthetized and mechanically ventilated. Injury was severe and comparable across all animals in the study (PaO_2/FIO_2 145 ± 11 mmHg). After baseline cardiopulmonary measurements a baseline P-V curve was obtained. After repeated saline lung lavage (mean 6.5 ± 0.7) to a PaO_2/FIO_2 ratio of less than 200 mmHg and volume history normalization a pressure volume curve was generated, and in vivo microscopy of the lung surface was performed. P-V curves and in vivo microscopy were obtained in five of the eight animals; three of the animals were discarded due to air leaks in the lung.

Anesthesia/surgical preparation

An intraperitoneal injection of ketamine (90 mg/kg) and xylazine (10 mg/kg) was used to induce an anesthetic state. Additional doses of ketamine/xylazine were administered if adequate anesthesia was not achieved, or if hypertension developed during experimentation. The right internal jugular vein was cannulated with a silastic catheter of 0.030 in. inner diameter. A 2.5-mm neonatal endotracheal tube was inserted through a tracheotomy, secured, and connected to the Galileo ventilator (Hamilton Medical, Reno, Nev., USA). After initiation of positive-pressure ventilation all animals were paralyzed with an intravenous dose of pancuronium (0.8 mg/kg). Mechanical ventilation was initiated in a pressure-control mode with 50% decelerating flow, a respiratory rate of 35/min, PEEP of 3 cmH_2O, and a tidal pressure of 14 cmH_2O. The tidal pressure was adjusted to maintain baseline tidal volume (10–12 cc/kg). The inspiratory-to-expiratory ratio was 1:2 in all groups. The fraction of inspired O_2 was 1.0. The respiratory rate was adjusted to prevent hypercarbia ($PaCO_2 > 45$). A thoracotomy was performed to accommodate the microscopic apparatus. To standardize lung volume history prior to the generation of each curve all animals received a minimum of three breaths with peak pressures of 40 cmH_2O and zero end-expiratory pressure.
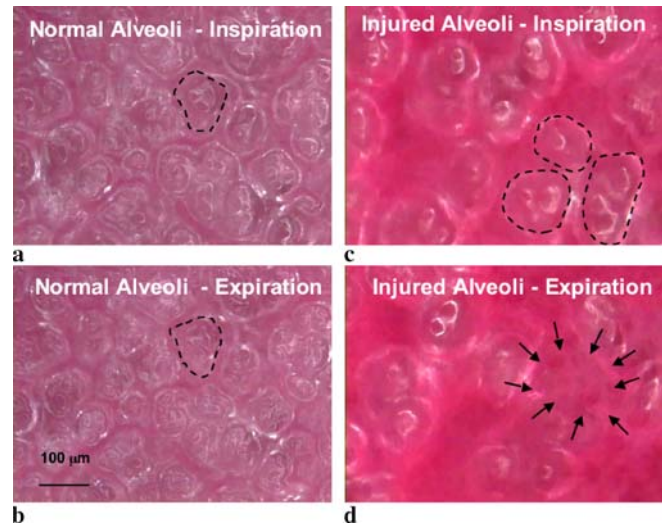
Lung injury

Normal saline was warmed to 38 °C and administered intratracheally at sequential doses of 16 ml/kg. Five initial doses were given and the PaO_2/FIO_2 was assessed after 15 min of interval ventilation. The respiratory rate was adjusted after each blood gas assessment to achieve a PCO_2 of 35–45 mmHg. Additional individual doses of saline were administered until the PaO_2/FIO_2 after 15 min of interval ventilation was below 200 mmHg.

Generation and analysis of quasistatic pressure-volume curve

The breathing circuit was opened to atmospheric pressure (altitude 364–681 ft). For the inflation limb sequential aliquots of room air were delivered by a programmable syringe (PHD 2000, Harvard Apparatus, Holliston, Mass., USA) with airway pressure being transduced at the end of the tracheal cannula (P75, Hugo Sachs Elektronik, Germany). These volume aliquots were delivered until the stable airway pressure exceeded 40 cmH_2O. Volume was then withdrawn in the same manner for generation of the deflation limb until the stable airway pressure approximated zero. No accommodation was made to adjust for temperature, pressure, or gas exchange. The P-V points for each limb were regressively fit to the general sigmoid equation [10] using a statistical software package (JMP 5.0.1, SAS, Cary, NC, USA): $V = a + \{b/[1 + e^{-(P-c)/d}]\}$. The resultant values of c and d from each fit were then used to determine the upper and lower inflection points on each limb. The points of maximal compliance increase and decrease for each limb were defined as the $LIP_{(I \text{ or } d)}$ and $UIP_{(I \text{ or } d)}$, respectively. Specifically, $LIP = c - 1.317d$ and $UIP = c + 1.317d$ [11].

In vivo videomicroscopy

The microscope (XDFM, Olympus, Orangeburg, N.Y., USA) accommodates a reflected light, brightfield illuminator (U-LH100UH, Olympus). Twelve distinct 1.0-mm^2 microscopic fields were selected on the anterior pleural surface of the right lower lobe. These fields were filmed at 5-cmH$_2$O increments with inflation from 0 to 40 cmH$_2$O and at 5 cmH$_2$O decrements with deflation back to 0 cmH$_2$O with the in vivo microscope. Microscopic images of the field were digitally recorded and alveolar silhouettes were outlined with the use of image analysis software (Fig. 1, Image Pro Plus 5.1, Media Cybernetics, Silver Springs, Md., USA). The number of alveolar silhouettes/microscopic field was used to measure alveolar recruitment and the size of the silhouettes to measure alveolar volume change. The index of alveolar recruitment (%R) was measured as the proportion of the microscopic field that contained inflated alveolar silhouettes. The number of recruited alveoli (#R) was measured as the number of alveolar silhouettes identified in the microscopic field at each inflation pressure. The alveolar derecruitment pressure (DP) was determined by direct visualization of alveolar collapse using the in vivo microscope, as the airway pressure was diminished incrementally from 40 cmH$_2$O. We used the mean of the 12 images at each pressure-step for each animal individually. Any comparison of recruitment across animals used the mean recruitment of the 12 images. The mean recruitment from each of these points was used in the generation of a pressure-recruitment curve that was fit to the generalized sigmoid equation for each animal. For each animal we compared the 12 images from each pressure-point on the deflation limb of the pressure-recruitment curve to the 12 images at 40 cmH$_2$O from the same animal to determine the derecruitment pressure. The DP is defined as the airway pressure at which a significant ($p < 0.05$) decrease in the %R occurred.

Fig. 1 a-d The same microscopic field at peak inspiration (**a**, **c**) and end expiration (**b**, **d**) in both the normal lung (**a**, **b**) and following injury by saline lavage (**c**, **d**). The same alveolus is seen (*circled by black dashes*) at inspiration (**a**) and expiration (**b**). Note the minimal change in size with ventilation in the normal lung. In the saline injured lung alveoli recruit and derecruit with each breath. At inspiration three alveoli are open in the lower right of the microscopic field (*outlined by dashes*). These alveoli collapse during expiration; *arrows* microatelectasis following alveolar collapse

Statistical analysis

Data for all interanimal comparisons passed for normalcy using the Shapiro–Wilk test ($p < W > 0.05$).

Table 1 Animal characteristics before and after saline lavage lung injury (*LIP* lower inflection point; *UIP* upper inflection point)
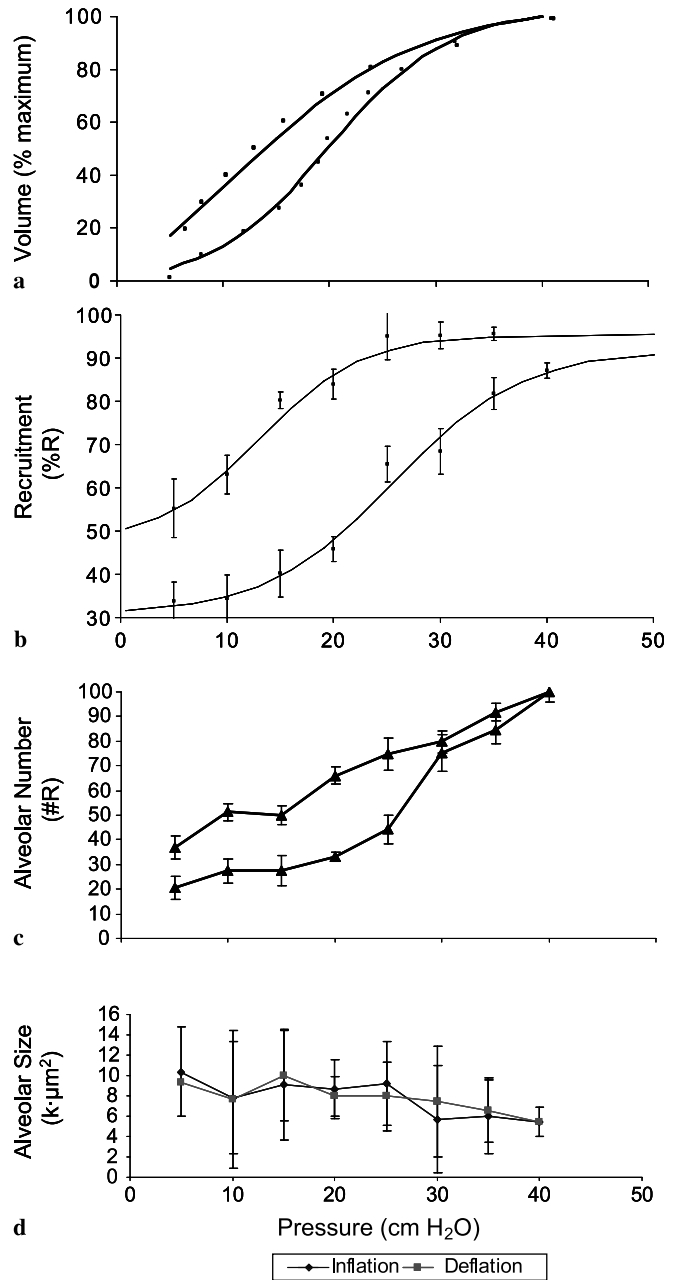
|	Baseline	Injury
Arterial pH	7.37 ± 0.02	7.20 ± 0.02*
Arterial blood carbon dioxide partial pressure	41 ± 2	39 ± 2
Arterial blood oxygen partial pressure	526 ± 19	145 ± 11*
Arterial blood oxygen saturation	98.8 ± 0.3	94.4 ± 0.8*
Hemoglobin	13.8 ± 0.6	11.8 ± 0.8
Mean arterial pressure (mmHg)	79 ± 7	73 ± 6
Respiratory rate (min^{-1})	25 ± 1	28 ± 1
Plateau pressure (cmH$_2$O)	17.3 ± 0.2	25.9 ± 2.4*
Mean airway pressure (cmH$_2$O)	5.8 ± 0.4	8.0 ± 0.8*
Positive end-expiratory pressure (cmH$_2$O)	3	3
Tidal volume (ml)	5.8 ± 0.3	5.9 ± 0.4
Mechanical ventilation	0.14 ± 0.01	0.16 ± 0.01
Inspiratory resistance (cmH$_2$O l^{-1} s^{-1})	63 ± 17	137 ± 36*
Static compliance (ml cmH$_2$O^{-1})	0.43 ± 0.02	0.29 ± 0.01*
LIP inflation limb (cmH$_2$O)	0.64 ± 0.67	14.4 ± 2.0
UIP deflation limb (cmH$_2$O)	12.0 ± 1.2	20.3 ± 1.5
UIP inflation limb (cmH$_2$O)	12.0 ± 0.9	26.7 ± 2.4

*$p < 0.05$ vs. baseline
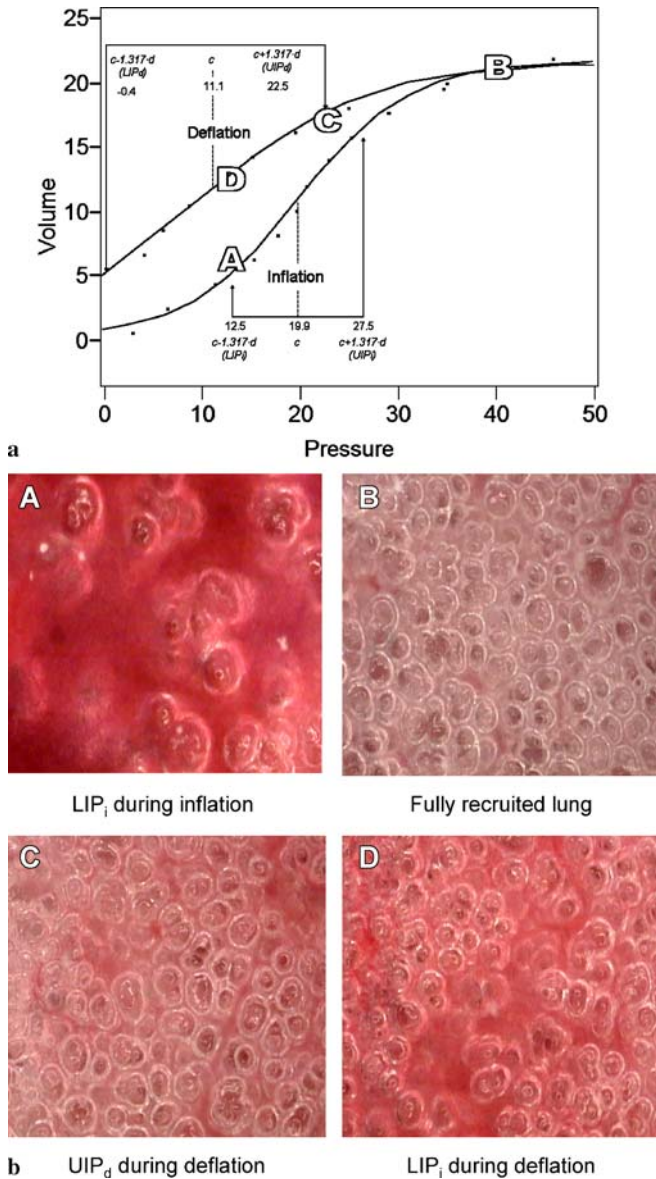
Fig. 2 a, b Individual data points (*dots*) in a single animal during lung inflation (*lower curve*) and deflation (*upper curve*) fit with the Venegas equation (*lines*). *A–D* The points on the curve corresponding to the airway pressures of the in vivo photomicrographs (**b**). The in vivo microscopic fields corresponding to the points on the P-V curve (**a**, *A–D*) and seen in **b** (*A–D*). At the lower inflection point only a few alveoli are recruited, and the majority of the microscopic field is atelectatic (*A*). At peak inflation the field is comprised entirely of inflated alveoli (*B*). During deflation at UIP_d alveoli remain inflated with no areas of microatelectsis (*C*). Further deflation of the lung to a pressure corresponding to the LIP_i (*D*) causes some alveolar collapse (*D*). An area of microatelectasis can be seen in the center of the microscopic field (*D*). Note, however, that there was significantly more microatelectasis at the LIP_i than at the same airway pressure on the deflation limb of the P-V curve (*A, D*)

Fig. 3 a-d Comparison of the morphology of normalized sigmoid curves relating airway pressure to lung volume (**a**) and total alveolar recruitment (%R, **b**). The number of visible alveoli per field (#R, **c**) and the size of alveolar silhouettes (**d**) are also shown. Changes in lung volume parallel change in alveolar recruitment (%R and #R). The size of alveolar silhouettes did not change significantly at any point across the entire inflation and deflation pressure range

All relevant data are expressed as mean $\pm$ SE. Significance of DP was determined by a two-tailed *t*-test. The degree of linear correlation (R^2) was calculated between the DP and the inflection points on the inflation and deflation limbs of all animals. Data regarding different pressure levels in an individual animal were compared using Student's *t*-test. Significance was set at $p < 0.05$.
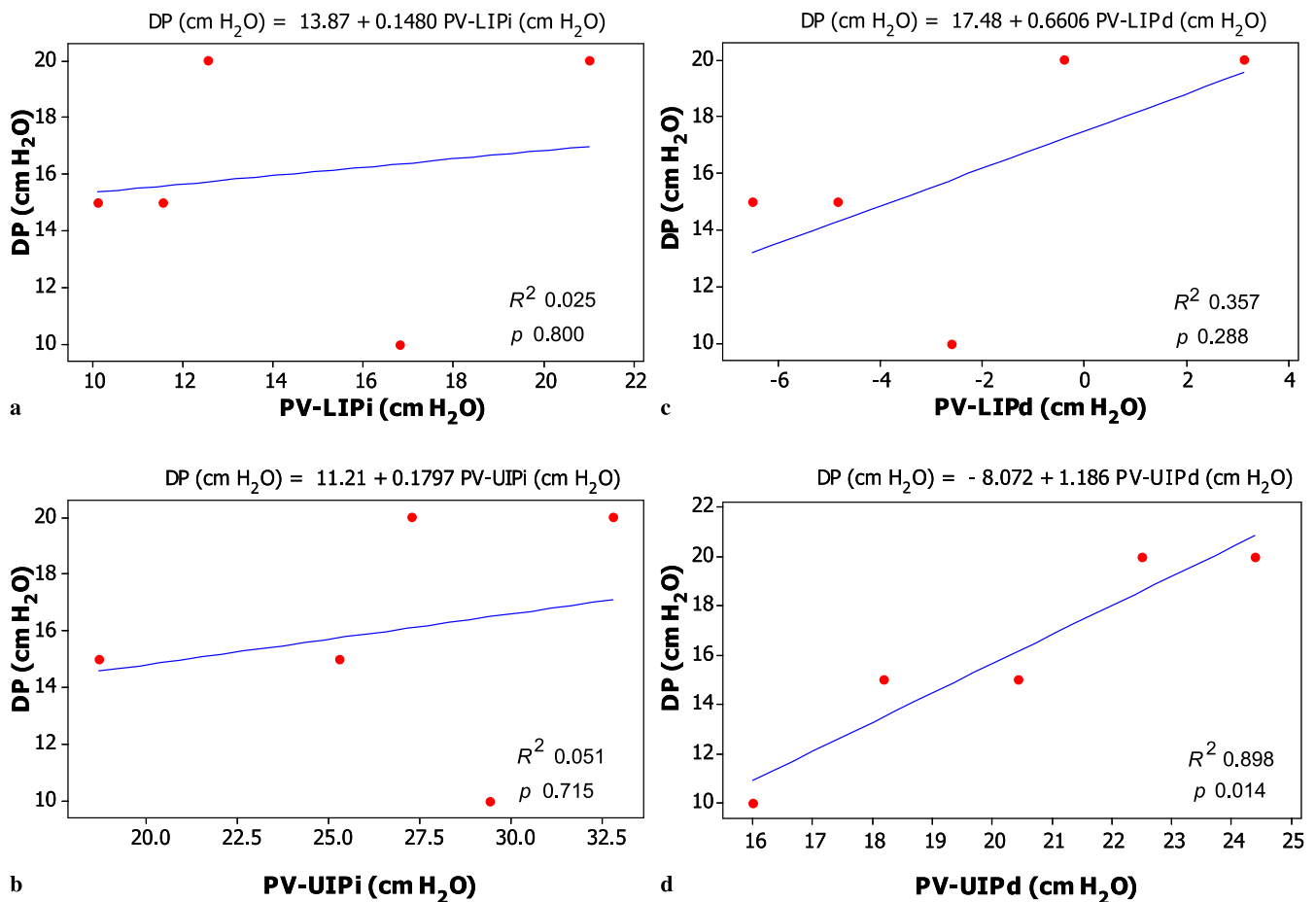
Fig. 4 a-d Correlation of P-V lower (*LIP*) and upper (*UIP*) inflection points with derecruitment pressure (*DP*). LIP UIP on both inflation (*i*) and deflation (*d*) were calculated using the Venegas et al. [10] equation. The correlation between these inflection points and DP was analyzed; only UIP_d was correlated well with DP

Results

Pressure-volume curves

Blood gas and pulmonary mechanics are found in Table 1. Fig. 2a presents the whole-lung P-V curve of a single animal during inflation (lower curve) and deflation (upper curve) fit with the equation of Venegas et al. [10] (see above) and corresponding in vivo microscopic images (Fig. 2b). All postinjury curves were adequately fitted to the P-V model (adjusted R^2: inflation 0.973 ± 0.006, deflation 0.981 ± 0.007). Airway pressures at LIP_i (14.4 ± 2.0 cmH$_2$O) were significantly less than those at UIP_d (20.3 ± 1.5 cmH$_2$O), which were consistently lower than those at UIP_i (26.7 ± 2.4 cm H$_2$O, $p < 0.05$). These calculated inflection points were all significantly greater than the corresponding inflection points of the P-V curves obtained prior to injury (Table 1). There was no significant difference in inflection points on the inflation and deflation limbs of the preinjured lung.

In vivo microscopy

Grossly, injury appeared to be homogeneous throughout the entire lung with this model. A DP was identified in all animals (16.0 ± 1.9 cmH$_2$O). There was significant alveolar collapse at 5 cmH$_2$O airway pressure on the both the inflation and deflation limb of both the pressure–alveolar recruitment (P-#R) and pressure–proportional alveolar recruitment (P-%R) curves (Fig. 3). At 40 cm H$_2$O alveolar recruitment greatly increased as demonstrated by the increase in both #R (77.2 ± 5.5 alveoli/field) and %R ($68.7 \pm 0.1\%$). There was a significant difference in alveolar recruitment (both #R and %R) between the inflation and deflation limbs at all airway pressures 25 cmH$_2$O and below ($p < 0.05$).
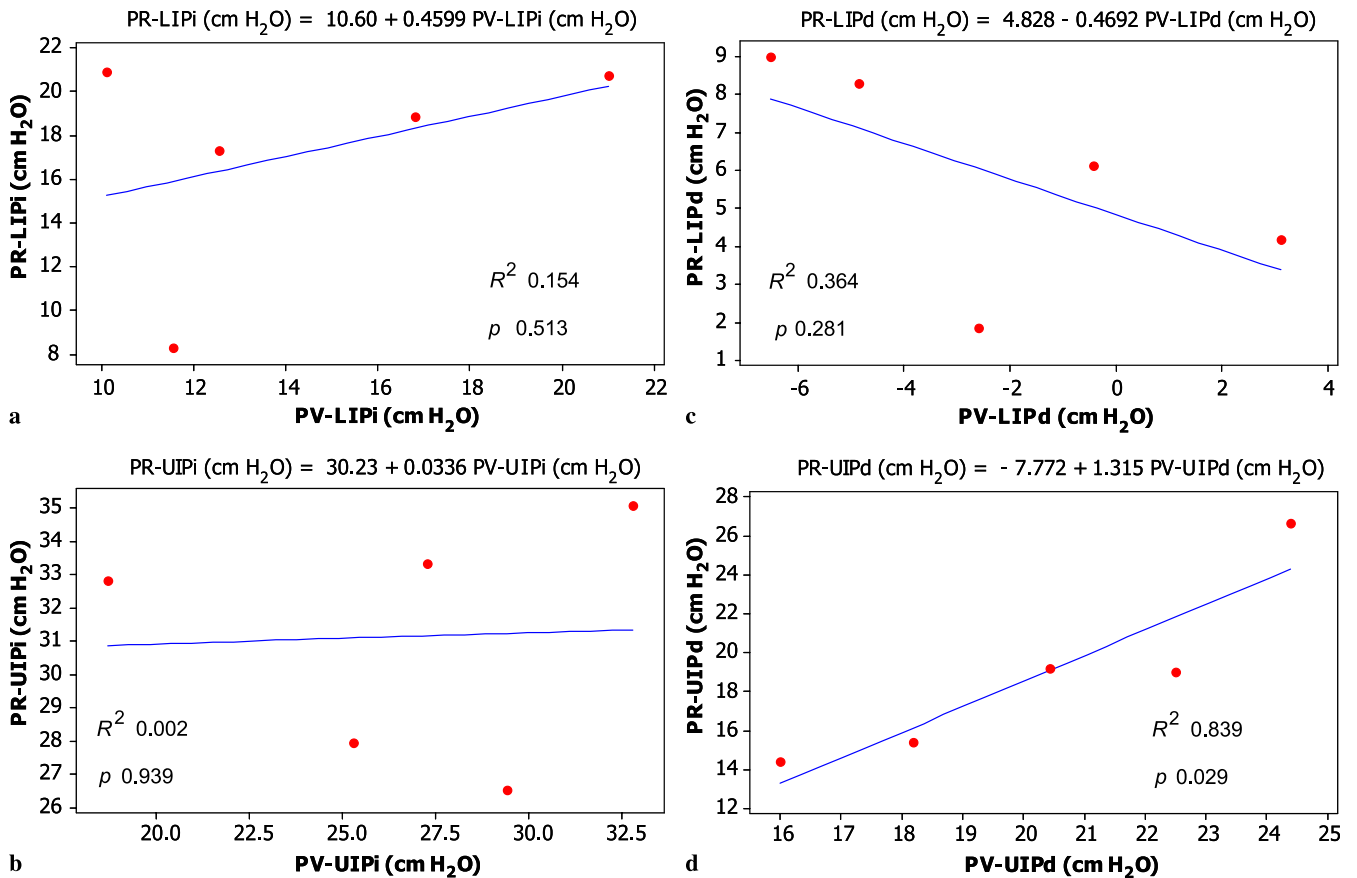
Fig. 5 a-d Correlation of P-V lower (*LIP*) and upper (*UIP*) inflection points with corresponding inflection points on the pressure-recruitment curves. LIP and UIP on both inflation (*i*) and deflation (*d*) were calculated using the Venegas et al. [10] equation. The correlation was analyzed between these inflection points and the corresponding pressure-recruitment inflection points derived from the same sigmoid equation fitting method. Only at UIP_d was there some correlation of the corresponding inflection points

There was no significant difference in alveolar size between any pressures on the inflation or deflation limbs (Fig. 3d). %R was closely correlated with #R ($R^2 = 0.928 \pm 0.032$).

Correlation of alveolar recruitment and lung volume

The degree of alveolar recruitment on the deflation limb was significantly higher at UIP_d than at LIP_i on the inflation limb (64.2 ± 2.7 vs. 47.3 ± 3.5). Poor correlation was found between LIP_i and DP whereas UIP_d and DP were closely correlated (Fig. 4). UIP_d was consistently 2.5–6.0 cmH$_2$O above the identified DP. There was a significant difference in recruitment at LIP_i between deflation and inflation (%R 47.3 ± 3.5 vs. $14.0 \pm 4.6\%$, $p < 0.05$). Recruitment continued above the UIP_i on the inflation limb (%R 45.4 ± 8.4 vs. 68.7 ± 0.1 at 40 cm H$_2$O, $p < 0.05$). P-%R curves were analyzed by fitting the data to a sigmoid equation; the P-%R curves fit the sigmoid equation well ($R^2 = 0.949$). We also examined the correlation between the calculated inflection points of the P-V and P-%R curves (i. e., LIP_i, UIP_i, LIP_d, UIP_d on P-V curve vs. those on the P-%R curve). There was very poor correlation between the pressures of each inflection point with the exception of UIP_d, which was more highly correlated ($R^2 = 0.839$, $p = 0.029$, Fig. 5).

Discussion

Critique of the methods

The purpose of this study was to determine whether the inflection points on the P-V curve are correlated with alveolar recruitment and derecruitment as originally hypothesized [12]. Specifically, we tested this hypothesis by directly visualizing individual alveolar opening and collapse and analyzed the correlation between this and calculated inflection points on the P-V curve. Although these data could be extrapolated to the clinical use of inflection points to set PEEP in patients with acute respiratory distress syn-

drome (ARDS), this was not the intension of the present study. Indeed, we chose an injury model (saline lavage) that is not a clinically accurate model of acute lung injury but does result in very unstable alveoli that readily collapse and reopen. The saline lavage injury model was appropriate for the question that we asked and answered in this study. However, there are other potential problems with the techniques used in this study.

There are several artifacts inherent with the technique of alveolar in vivo microscopy. The chest must be open to attach the microscope negating the negative intrathoracic pressure. This may alter the absolute changes in alveolar size and number at any given airway pressure. However, the relative changes in alveolar mechanics during lung inflation and deflation should not be affected. Also, we observed alveoli only on the nondependent lung. It is possible that alveolar recruitment and derecruitment could be at different points on the P-V curve on the dependent vs. the nondependent lung.

Use of the pressure-volume curve

Several studies have used P-V curves as a tool to estimate changes in alveolar size or state of recruitment [1, 4, 6, 7]. Without being able to directly visualize alveoli, Amato et al. [1] interpreted the LIP_i as the point on the P-V curve where the majority of alveoli are recruited; they found that alveoli increased in size during the straight portion of the P-V curve, and that alveoli were beginning to over distended above the UIP_i. However, this interpretation of alveolar mechanics has been challenged from both a theoretical [2–4] and an experimental [5–9, 13] perspective.

A pair of studies demonstrated that alveoli recruit throughout lung inflation in an animal model of ARDS [1] and in ARDS patients [8] using computed tomography. These authors concluded that recruitment is an inspiratory phenomenon that occurs along the entire inspiratory limb of the P-V curve, and that end-expiratory alveolar collapse is a component of both the preceding lung inflation (recruitment maneuver) and the end-expiratory pressure. In addition to P-V curves, Downie et al. [13] added small-volume tidal P-V loops (simulated tidal breaths) to measure tidal R/D in relation to the position on the P-V curve. They observed that tidal recruitment occurred when the peak pressure was above the point of slope change on the inflation limb and that recruitment continued up to $40 \, cmH_2O$. This tidal recruitment was minimized after reducing PEEP from a recruited state. The disparity between their measurements before and after recruitment supports the concept of using the deflation limb. Lastly, Albaiceta et al. [9] performed computed tomography sequentially on both the inflation and deflation limb of the P-V curve in patients with early lung injury. They found that the volume of aerated lung based on tissue density continuously increased during inflation and that the aerated lung during deflation only dropped significantly at pressures below the point of maximum curvature on the deflation limb of the P-V curve.

The results of this study support the concept of alveolar recruitment throughout lung inflation, minimal alveolar derecruitment with deflation until a critical closing pressure is reached at which time there is a progress alveolar collapse. In addition, direct visualization of alveoli in this study suggests that there is not a massive alveolar recruitment at the LIP_I, that alveoli do not expand in size during the flat portion of the inflation curve but rather increased in number, and that alveoli do not overdistend above the UIP_i (Fig. 3d). On deflation there was minimal change in alveolar number until below the UIP_d, at which time a significant derecruitment occurred; little change in alveolar size is seen during deflation (Table 1).

Hickling [2, 3] published two papers using a mathematical model to interpret the shape and location of the infections points on the P-V curve. His original model incorporated gravitational superimposed pressure, alveolar threshold opening pressures and PEEP to predict changes in the slope of the P-V curve and inflections points. In Hickling's model the superimposed pressure influenced the LIP_i more than the thresholds, and the LIP_i did not accurately predict optimum PEEP (to prevent end-expiratory collapse of alveoli). The linear portion of the curve was characterized by continual alveolar recruitment. The model demonstrated that alveolar recruitment could occur past the UIP_i, which would render the UIP no longer representative of the point of alveolar over distension [2]. Although recruitment occurs past the UIP_i, this does not eliminate the possibility that over distension and injury may also be occurring. A modification of this model was used to simulate incremental and decremental trials for optimal PEEP [3]. Hickling found that the PEEP, which produced maximal compliance during incremental PEEP, was not correlated with the optimal PEEP. Maximal compliance during a decremental PEEP trial was, however, predictive of optimal PEEP. This conclusion is supported by our data which identified decremental or deflation-related characteristics to be more predictive of alveolar derecruitment.

Jonson et al. [5] demonstrated a high compliance on the inflation limb of the P-V curve in patients with acute lung injury which suggested that alveolar recruitment was occurring above the LIP_i. This supports the data from the mathematical models [2, 3] and suggests that neither the LIP_i nor the slope of the inflation limb of the P-V curve is likely to specify optimal PEEP. Although alveolar recruitment and derecruitment is the likely mechanism for these changes in the P-V curve, the possibility exists that surfactant film hysteresis plays a role that cannot be excluded.

Our data support the conclusions of Jonson et al. [5] and Hickling [2, 3] as we directly observed alveolar recruitment on inflation and derecruitment on deflation and

also demonstrated significant alveolar recruitment above the LIP$_i$. However, a major difference in our experimental model from either Hickling's mathematical model or Jonson's clinical study was that our recruitment curves were generated in open-chest rats and on alveoli limited to the nondependent lung. Thus gravitational pressure is always equal to zero without interframe variation.

The shape of the whole-lung pressure volume curve is determined by: (a) viscoelastic properties of the lung, (b) chest wall compliance, (c) alveolar surface tensions mediated by pulmonary surfactant function, and (d) intra-alveolar contents. The sigmoid morphology of the P-V could possibly be explained by a combination of these effects. The present study indicates that the sigmoid morphology of the pressure-recruitment curves persists despite the elimination of chest wall compliance and gravitational pressure. We have previously demonstrated that there is little or no change in alveolar recruitment in the naive lung over clinically applicable pressure ranges [14]. Thus changes in volume in the naive lung appear to be related to changes in conformation and volume of alveoli rather than by changes in the state of recruitment. Despite the apparent lack of recruitment/derecruitment in the

naive lung the P-V curve remains sigmoidal in nature. The most significant difference after surfactant deactivation by saline lavage is that the curve shifts to the right (increase in inflection point pressures) without significant change in the width of the curves. It appears therefore that the increased surface tension associated with loss of surfactant function is solely responsible for the increase in inflection point pressures.

Conclusions

In the saline lavage injured lung recruitment occurs throughout the entire inflation limb of the P-V curve. On the deflation limb more alveoli remain open at a similar pressure as compared to the inflation limb (hysteresis). The calculated LIP on the inflation limb was not correlated with the alveolar recruitment whereas the UIP on the deflation was correlated with alveolar derecruitment. The implications of this study are that (a) alveolar recruitment and derecruitment take place at different pressures, and (b) the use of deflation limbs of P-V curves has greater inference to alveolar derecruitment than inflation limbs.

References

1. Amato MB, Barbas CS, Medeiros DM, Magaldi RB, Schettino GP, Lorenzi-Filho G, Kairalla RA, Deheinzelin D, Munoz C, Oliveira R, Takagaki TY, Carvalho CR (1998) Effect of a protective-ventilation strategy on mortality in the acute respiratory distress syndrome. N Engl J Med 338:347–354

2. Hickling KG (2001) Best compliance during a decremental, but not incremental, positive end-expiratory pressure trial is related to open-lung positive end-expiratory pressure: a mathematical model of acute respiratory distress syndrome lungs. Am J Respir Crit Care Med 163:69–78

3. Hickling KG (1998) The pressure-volume curve is greatly modified by recruitment. A mathematical model of ARDS lungs. Am J Respir Crit Care Med 158:194–202

4. Frazer DG, Lindsley WG, Rosenberry K, McKinney W, Goldsmith WT, Reynolds JS, Tomblyn S, Afshari A (2004) Model predictions of the recruitment of lung units and the lung surface area-volume relationship during inflation. Ann Biomed Eng 32:756–763

5. Jonson B, Richard JC, Straus C, Mancebo J, Lemaire F, Brochard L (1999) Pressure-volume curves and compliance in acute lung injury: evidence of recruitment above the lower inflection point. Am J Respir Crit Care Med 159:1172–1178

6. Schiller HJ, Steinberg J, Halter J, McCann U, Dasilva M, Gatto LA, Carney D, Nieman G (2003) Alveolar inflation during generation of a quasi-static pressure/volume curve in the acutely injured lung. Crit Care Med 31:1126–1133

7. Pelosi P, Goldner M, McKibben A, Adams A, Eccher G, Caironi P, Losappio S, Gattinoni L, Marini JJ (2001) Recruitment and derecruitment during acute respiratory failure: an experimental study. Am J Respir Crit Care Med 164:122–130

8. Crotti S, Mascheroni D, Caironi P, Pelosi P, Ronzoni G, Mondino M, Marini JJ, Gattinoni L (2001) Recruitment and derecruitment during acute respiratory failure: a clinical study. Am J Respir Crit Care Med 164:131–140

9. Albaiceta GM, Taboada F, Parra D, Luyando LH, Calvo J, Menendez R, Otero J (2004) Tomographic study of the inflection points of the pressure-volume curve in acute lung injury. Am J Respir Crit Care Med 170:1066–1072

10. Venegas JG, Harris RS, Simon BA (1998) A comprehensive equation for the pulmonary pressure-volume curve. J Appl Physiol 84:389–395

11. Harris RS, Hess DR, Venegas JG (2000) An objective analysis of the pressure-volume curve in the acute respiratory distress syndrome. Am J Respir Crit Care Med 161:432–439

12. Steinberg J, Schiller HJ, Halter JM, Gatto LA, Dasilva M, Amato M, McCann UG, Nieman GF (2002) Tidal volume increases do not affect alveolar mechanics in normal lung but cause alveolar overdistension and exacerbate alveolar instability after surfactant deactivation. Crit Care Med 30:2675–2683

13. Downie JM, Nam AJ, Simon BA (2004) Pressure-volume curve does not predict steady-state lung volume in canine lavage lung injury. Am J Respir Crit Care Med 169:957–962

14. DiRocco JD, Pavone LA, Carney DE, Lutz CJ, Gatto LA, Landas SK, Nieman GF (2006) Dynamic alveolar mechanics in four models of lung injury. Intensive Care Med 32:140–148